Medyawanti Pane (Analysis of the Effect of Calcination Time on Microstructure, Functional Groups, and Crystal Structure of LiNiO2 Battery Cathode Material)

by Library Referensi

Submission date: 20-Feb-2025 12:20PM (UTC+0700)
Submission ID: 2592697625
File name: ps,_and_Crystal_Structure_of_LiNiO2_Battery_Cathode_Material.pdf (1.47M)
Word count: 4643
Character count: 24839

VANOS
JOURNAL OF MECHANICAL ENGINEERING EDUCATION
http://jurnal.untirta.ac.id/index.php/vanos
ISSN 2528-2611, e-ISSN 2528-2700
Volume 7 Number 1, May 2022, Pages 67-78

Analysis of the Effect of Calcination Time on Microstructure, Functional Groups, and Crystal Structure of $LiNiO_2$ Battery Cathode Material

Budiarto[1], Edward Baringin Oloan Sihite[2], Medyawanti Pane[3]

[1,2,3]Department of Mechanical Engineering, Universitas Kristen Indonesia, Indonesia
Mayjen Sutoyo Street No.2, Cawang, Kec. Kramat Jati, Kota Jakarta Timur,
Daerah Khusus Ibukota Jakarta 13630

Corresponding author: budiarto@uki.ac.id

Received: 04 March 2022. Accepted: 03 April 2022. Published: 01 May 2022

ABSTRACT

Battery cathode material is one of the four determinants of energy storage capacity, which is used as a power source in electronic equipment. laptops, and electric vehicles. Synthesis of the cathode material for $LiNiO_2$ battery with one stage co-precipitation method, and variations in calcination time of 3, 6, 9 and 24 hours with a constant temperature of 700^{0}C. Microstructure observations with SEM showed an uneven and homogeneous surface. The elemental compositions of Li, and Ni were analyzed by EDXS showing that Li and Ni metal decreased with increasing calcination time. The results of the crystal structure test using an X-ray diffractometer showed that with increasing calcination time the crystallite diameter decreased, but the dislocation density increased. The micro-lattice strain increased with increasing calcination time in the planes of the Miller hkl index (102), (104), (210), (108), and (113). The FTIR spectra show that the peak at wavenumber 433 cm^{-1} is caused by the asymmetric stretching vibration of Li–O in LiO_6 and bending vibration of NiO_6, namely [(Ni–O–Li)], appearing at 603 cm^{-1}.

Keywords: LNO battery cathode, microstructure, FTIR, XRD, SEM-EDXS

INTRODUCTION

The largest nickel ore content in the world is in the form of laterite and limonite nickel ore minerals, the reserves of these mineral sources are more than 23.7% located in Indonesia, especially the islands of Sulawesi and Maluku, as well as other islands. Until now, the largest supplier of energy in Indonesia is from fossil fuels, which are increasingly depleting. For this reason, the government has planned to provide mixed energy, one of which is new and renewable energy, such as hydroelectric power plants, wind power plants, geothermal power plants, and solar panel power plants. The Wave power plant, and so on. New renewable energy to reduce CO_2, SO_X, NO_X emissions, which cause global warming. The Indonesian government has built a mineral processing plant for laterite nickel ore and limonite into stainless steel and lithium-ion batteries (BLI). BLI is one of the energy storage components in electric cars that will be produced in the Sulawesi area. It requires human resources and infrastructure as well as large costs. The component that cannot be separated from the increasing demand for electrical energy is the energy storage device itself (energy storage). Energy storage is generally known as an accumulator or battery. The most dominant type of battery is a rechargeable battery, one of which is the lithium-ion battery [1].

A lightweight, rechargeable battery. Batteries are now widely used in all aspects of life, from cell phones to electric vehicles. Batteries can also store large amounts of energy from renewable energy sources such as solar and wind power so that they can replace the use of fossil fuels.

The main components of the battery consist of a cathode (oxidation electrode), anode (reduction electrode), electrolyte as a lithium-ion transfer medium, and a separator as an electrode separator and electrolyte transfer path. The electrode is given a current collector which has a high conductivity to flow current from or to the electrode during the charging and discharging process. In the discharge process, lithium ions move from the anode to the cathode and change chemical energy into electrical energy. For the charging process, lithium ions move from the cathode to the anode and there is a change in electrical energy into chemical energy [2].

The advantages of lithium ion-based batteries are that they are the lightest metal and have the highest electrochemical potential compared to other metals. Lithium is the lightest metal element and has a very low redox potential [E(Li*/Li)=-3.04 V vs SHE)], which allows cells to have high voltages and high energy density and can provide a specific capacity of 3,600 Ah/kg. This value is much larger than the typical capacity of the secondary lead-acid type battery which is 260 Ah/kg. The disadvantage of lithium-ion batteries is that they are damaged when used below 2 volts and evaporate when they are overvoltage.

Therefore, lithium-ion batteries generally use circuit management devices and mechanical breakers to protect over-discharge or over-temperature conditions, in addition, they lose permanent capacity at high temperatures (65 ^{0}C)[3][4].

There are several types of lithium-based secondary batteries currently being developed, including lithium-ion batteries, lithium polymer batteries, and lithium-sulfur batteries. Lithium is also highly reactive to water and oxygen, so lithium batteries must use electrolytes that do not contain water such as lithium hexafluorophosphate ($LiPF_6$), Lithium tetrafluoroborate ($LiBF_4$), and Lithium perchlorate ($LiClO_4$), all of which are dissolved in organic solvents[4][5].

The cathode is the most important part of the battery and half the cost of producing the battery is the price of the cathode. Cathodes are classified into 3 based on their crystal structure, namely: layered, spinel, and olivine. $LiCoO_2$ is an example of a battery with a layered structure, in which lithium-ion transfer occurs in 2 dimensions. For spinel structure, ion transfer is carried out in 3 dimensions, an example of a commercial cathode with a spinel crystal structure is $LiMn_2O_4$. While the crystal structure of olivine, ion transfer occurs in 1 dimension, an example of a commercial cathode is $LiFePO_4$ [5].

Other positive electrode materials that have been introduced include $LiMn_2O_2$, $Li(NiMnCo)O_2$, $Li(NiCoAl)O_2$, and so on. In the future use of battery cathode materials, metal-based cathode materials have the opportunity to provide optimal results. Another supporting property for the use of anode material is the nanostructure which will affect the greater energy density. For this reason, research will be carried out on the manufacture of lithium-ion battery cathode material, namely $LiNiFeCoO_2$ (NFC)[6][7].

BIU materials consist of BLI anode and BLI cathode materials, which have a significant influence on the electrochemical properties and safety of lithium batteries. BLI cathode material has a role in accelerating secondary BLI adaptation. The results of previous studies that $LiFePO_4$ compounds as cathode materials for traditional lithium-ion batteries have low energy density[8]; the compound lithium cobalt dioxide ($LiCoO_2$) has excellent electrochemical performance, but cobalt is rare and toxic[9]; which is a compound of lithium nickel dioxide ($LiNiO_2$) mixing series cations Ni^{2+} and Li^+ and irreversibly high capacity[10]. And the layered lithium manganese dioxide ($LiMnO_2$) compound has a crystallographic transformation that has a spinel structure[3][4].

Analyze crystallite structure and density of line deformities (dislocations)

The X-ray diffractogram pattern is formed from the interaction between the X-ray beams hitting the $LiNiO_2$(LNO) battery cathode material sample, if the LNO battery cathode material test sample has a sequential

structure, then some x-ray beams will change direction at their angle depending on from the structure of the test material, the sample material for the LNO battery cathode and the wavelength of the x-ray radiation source used. For this reason, it can be determined whether an LNO battery cathode material has a high density or not, and pictures and analysis using XRD tools for testing samples of LNO battery cathode material can be seen below.

How to determine the X-ray diffraction angle from the results of the LNO battery cathode material test, can be determined by the Bragg law equation, namely:

$n\lambda = 2\, d_{hkl} \sin \theta_{hkl}$

where: n = is the order of diffraction

λ = wavelength of x-rays

d_{hkl} = distance between diffraction planes with millerhkl. index

θ = Bragg diffraction angle for the diffraction plane

From this equation, it can be seen that if the wavelength of the x-rays used is known and the angle θ_{hkl} is measured, it is possible to determine the distance between the diffraction planes d_{hkl}. For the cubic structure the distance d of the diffraction plane is related to the lattice parameters of the crystal structure by the following equation:

$$d_{hkl} = \frac{a}{\sqrt{h^2 + k^2 + l^2}}$$

where: a = lattice parameter

hk = miller index field

d_{hkl} = distance between planes

To determine and analyze the size/diameter of crystallites referring to the X-ray diffraction peaks of the diffractogram pattern using the Debye Scherrer equation approach which is formulated:

$$D = \frac{K\lambda}{\beta \cos\theta}$$

Meanwhile, to determine the value of the lattice strain, the formula is used:

$$\varepsilon = \frac{\beta}{(4\tan\theta)}$$

To determine the value of dislocation density, the formula is used:

$$\varepsilon = \frac{\beta}{(4\tan\theta)}$$

Where: D = Diameter of crystallite

ρ = Dislocation Density

ε = Lattice Strain

K = Form factor of the crystal (0.9-1)

λ= Wavelength of X-rays (1,54056)

β= Value of Full Width at Half Maximum (FWHM) (rad)

θ= diffraction angle (degrees)

Analyze surface morphology and chemical element composition with SEM-EDXS

Observation of the surface morphology or microstructure of the LNO material samples was used with the SEM-EDXS tool. In the principle of testing the SEM-EDXS tool, two types of electrons are known, namely primary electrons and secondary electrons. The primary electron material that has high energy is usually nickel, tungsten and platinum elements as well as secondary

electrons that will be captured by the detector, so that 2 types of electrons will convert the signal into an image signal.

In this study, it is hoped that with variations in calcination time, optimal microstructure data will be obtained in overcoming the problem of lithium nickel dioxide compounds as the cathode material for $LiNiO_2$ batteries.

RESEARCH METHOD

The implementation of this research/experiment took place in the Mechanical Engineering laboratory Faculty of Engineering, Universitas Kristen Indonesia, starting from the weighing of samples, the synthesis process, the sample molding process, and the calcination process. Variation of calcination time: 3, 6, 9, and 24 hours, and at a temperature of fixed 700 ^{0}C.

Ingredient

The materials used include: compound $Ni(NO_3)_2.6H_2O$, lithium hydroxide [LiOH], and egg white (a chelating agent), all materials used are of technical quality, as well as materials for complete metallography.

Equipment

The tools used include:

a. Complete sample making equipment (press and dies, ball mill/mixer)
b. Furnace (Thermoline)
c. SEM-EDXS Tool
d. X-ray diffractometer (XRD)
e. Analytical Scales
f. Complete metallographic equipment, example : grinding, polishing, and compacting.

Figure 1. Furnace heating device

Figure 2. X-Ray diffractometer machine

Figure 3. SEM-EDXS Machine

Figure 4. FTIR Spectrophotometry machine

Ways of Working

$LiNiO_2$ nanoparticles were made by mixing the $Ni(NO_3)_2.6H_2O$ compound with the LiOH compound, which was previously weighed and dissolved in a 1:1 ratio, added egg white, and aqua dest water solution. Egg white as a chelating agent to increase the reaction rate and combine Li and nickel ions to produce nanoparticles[5][11]. The solution was mixed for 3 hours through a stirrer at room temperature of 30°C. The above solution was dried at 110°C for 24 hours and then heated at 220°C. The gel obtained was ground and calcined at a constant temperature of 700°C with variations in calcination time of 3, 6, 9, and 24 hours under atmospheric conditions. The synthesized sample will be tested for microstructure and elemental composition utilizing SEM-EDXS, for testing the crystal structure includes: - dislocation density, lattice strain, and crystallite size using XRD. XRD test using CuK-α as a light source by applying a scanning speed of 20/minute at an angle range of 10^0 to 90^0. Functional group testing using FTIR.

RESULT AND DISCUSSION

Analysis of crystallite diameter, dislocation density, micro-strain with XRD on $LiNiO_2$ battery cathode material

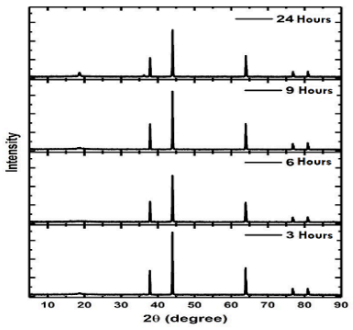

Figure 5. X-ray diffractogram of the $LiNiO_2$

Battery cathode material variations in calcination time, 3, 6, 8, and 24 hours, the temperature remains 700^0C.

Table 1. Relationship of hkl field, calcination time to diameter $LiNiO_2$ battery cathode material crystallite

Angle 2θ (^{0})	Miller Index (hkl)	Crystallite Diameter (nm)			
		Calcination time 3 hours	Calcination time 6 hours	Calcination time 9 hours	Calcination time 24 hours
37.92	(102)	7.1849	2.8740	1.7899	0.5992
44.16	(104)	4.7372	4.7372	4.1058	0.4895
64.31	(210)	4.2558	4.2558	4.2558	0.6989
76.98	(108)	2.9733	1.8813	1.9733	0.9864
81.21	(113)	5.3293	3.6179	3.2468	2.3657
Average		4,8961	3,4732	3,0743	1,0279

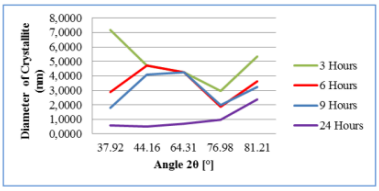

Figure 6. Graph of crystallite diameter relationship to angle 2 θ (⁰), variation calcination time 3, 6, 9, and 24 hours, fixed temperature 700⁰C

Table 2. Relationship of hkl plane, calcination time to strain $LiNiO_2$ battery cathode material micro lattice

Angle 2θ (⁰)	Miller Index (hkl)	Micro Grating Strain (%)			
		Calcination time 3 hours	Calcination time 6 hours	Calcination time 9 hours	Calcination time 24 hours
37.92	(102)	3.3775	5.0662	8.4437	40.5397
44.16	(104)	0.4817	0.3212	0.4817	12.6401
64.31	(210)	1.5431	1.5431	1.5431	10.1210
76.98	(108)	4.1129	4.1129	6.5000	13.4919
81.21	(113)	0.9132	1.1459	1.3451	2.2471
Average		2,0857	2,4378	3,6627	15,8079

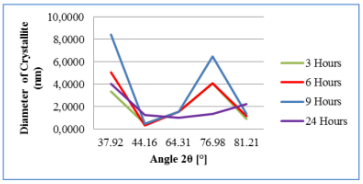

Figure 7. Graph of micro-lattice strain relationship to angle 2 θ (⁰), variation calcination time 3, 6, 9, and 24 hours, fixed temperature 700⁰C

Table 3. Relationship of hkl field, calcination time to density $LiNiO_2$ battery cathode material dislocation

Angle 2θ (⁰)	Miller Index (hkl)	Micro Grating Strain (%)			
		Calcination time 3 hours	Calcination time 6 hours	Calcination time 9 hours	Calcination time 24 hours
7.92	102)	0.0194	0.1211	0.0436	2.9302
4.16	104)	0.0446	0.0446	0.0398	2.5760
4.31	210)	0.0552	0.0552	0.0552	2.3752
6.98	108)	0.1131	0.2825	0.1131	1.2173
1.21	113)	0.0352	0.0764	0.0854	0.2132
Average		0,0535	0,1159	0,0674	1,8629

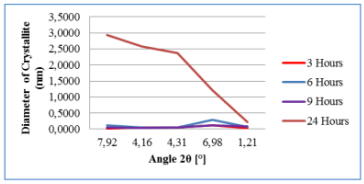

Figure 8. Graph of the relationship of dislocation density to angle 2θ (⁰), variation calcination time 3, 6, 9, and 24 hours, fixed temperature 700⁰C

The data obtained from the test results of crystallite diameter, micro-lattice strain, and dislocation density of the $LiNiO_2$ battery cathode material using an X-ray diffractometer (XRD), can be seen in Figure 5, and Tables 1, 2, and 3. diffraction to angle 2θ from a variation of calcination time 3, 6, 9, and 24 hours. Also, the relationship between crystallite diameter, micro-lattice strain, and discoloration density to the Miller index plane (hkl) ie (102), (104), (210), (108),

(113) and the calcination temperature remained at 700^{0}C.

From Figure 5, and Table 1, the results of the XRD test, show the diffractogram pattern according to the $LiNiO_2$ of α-$NaFeO_2$ rhombohedral system structure with space group R3m [11]. The formation of single-phase compounds showed that all observed peaks could be indexed in crystallite diameter, crystallite diameter distribution, and cathode material morphology. $LiNiO_2$ battery as well. Grain growth at a longer calcination time leads to smaller grain diameter. The average crystallite diameter for $LiNiO_2$ from the calcination time of 3 hours to 24 hours was 4.89 nm, reducing its size to 1.02 nm. The size of the crystallite diameter is evenly below 10 nm, which indicates high crystallinity. Previous researchers said that the battery cathode material made with smaller crystallite diameter sizes with high capacity and uniform crystallite diameter size distribution improved the overall battery performance with the uniform charge depth of each crystallite [12].

Table 1, also shows that the largest crystallite diameter in the Miller index plane (102) and angle 2θ= 37.92^0, calcination temperature of 700^{0}C and holding time of 3 hours, at 7.18 nm, and the smallest crystallite diameter in the Miller index field (104). angle 2θ = 44^0 is 0.48 nm. Table 2 shows that the largest micro-lattice strain is in the Miller index (102), angle 2θ = 37.92^0, at a calcination temperature of 700^{0}C with a holding time of 24 hours, which is 40.55 %. And the smallest micro-lattice strain in the Miller index (104), angle 2θ = 44^0, calcination temperature of 700^{0}C, and holding time of 6 hours, is 0.32%. When viewed from the parameter ratio of the highest diffraction peak intensity and the Miller index field (003)/(104) is small, this indicates the low content of Ni^{2+} ions in the $LiNiO_2$ sample. Because the presence of the element Ni^{2+} causes the position of the element Lithium (Li) to be swapped with the element Ni^{2+} so that the wrong atomic position can reduce the ability to move lithium ions and reduce the capacity of the battery. In addition, the presence of nitrate ions (NO3) can help the oxidation process from Ni^{2+} to Ni^{3+} so that the phenomenon of the exchange of Li and Ni elements can be inhibited[11].

Table 3 shows the value of the largest dislocation density in the Miller index (102), angle 2θ = 37.92^0, at a calcination temperature of 700^{0}C with a holding time of 24 hours, which is 2.9 lines/mm^2. And the smallest dislocation density, the same in the field of Miller index (102) and angle 2θ = 37.92^0, calcination temperature 700^{0}C holding time 3 hours, of 0.019 lines/mm^2, this indicates that the cathode material of $LiNiO_2$ battery after the calcination process has slight crystal defects.

The diffraction peak in the Miller index (108) or (003) has a very low intensity at the calcination temperature of 700^{0}C which indicates a transformation of the cubic crystal

structure[13]. The purity and crystallinity of $LiNiO_2$ nanopowder can be increased by calcination in an oxygen atmosphere and/or at temperatures higher than 700^{0}C[14][15].

Functional group analysis by FTIR on the cathode material $LiNiO_2$

Figures 9a, and 9b below, shows the spectrum of the cathode material for $LiNiO_2$ (LNO) batteries at calcination time variations of 6 hours, and 24 hours and a constant temperature of 700^{0}C with FTIR displayed through the relationship between wavenumber and absorption value. Wavenumber is a value that indicates the type of bond and absorbance is defined as the amount of absorption carried out by compounds that have certain bonds.

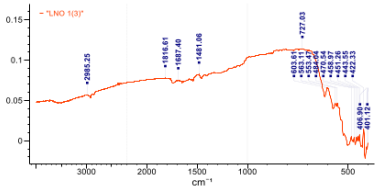

Figure 9. Spectrogram of $LiNiO_2$ battery cathode material during calcination 6 hours and a constant temperature of 700^{0}C

The peak of 1481 cm $^{-1}$ is the absorption of the H_2O bond vibration. There is no indication of other bonding from the previous hypothesis, namely the presence of impurities from other substances. From the absorption peak, it turns out that the cause of hydration of the LNO battery cathode material powder is from the bonding of the –OH hydroxyl functional group on the surface of the LNO particles. When the LNO battery cathode material powder has been calcined at a temperature of about 700^{0}C and removed from the furnace, it will interact with H_2O in the surrounding air. According to other researchers, the FTIR spectrum is in the form of a band. The band was found to be around 551-603 cm^{-1} for Li-O stretching vibrations, indicating the formation of LiO_6 octahedra[12]. The characteristic vibration of the metal oxide Ni-O, at the wavenumber, is 516-599 cm^{-1}. In a previous study, the wavenumber located around 638.36 cm^{-1} was associated with asymmetric stretching of the MO6 group mode (MNi, Mg, Co, and Zn)[12][16]. In addition, FTIR spectrum analysis can be used to determine the crystal structure and perfection of $LiNiO_2$ nanopowders. Where the FTIR spectrum shows the vibration mode correlated with the vibrations of the NiO_6 and LiO_6 octahedral units in the 400 - 700 cm^{-1} region[17]. Thus, the peak around 433 cm^{-1} is caused by the Li–O asymmetric strain vibration of LiO_6 and the NiO_6 bending vibration, namely [(Ni–O–Li)], appearing at 603 cm^{-1}.

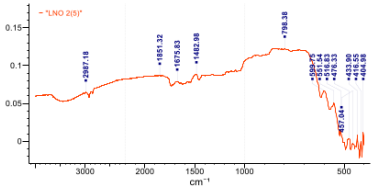

Figure 10. Spectrogram of $LiNiO_2$ battery cathode material during calcination 24 hours and a constant temperature of 700^{0}C

Analysis of microstructure and chemical element composition with SEM-EDXS on the cathode material $LiNi_{0,7}Fe_{0,2}Co_{0,1}O_2$

Figure 11 and 12, the surface morphology of the $LiNiO_2$ battery cathode materials, shows that the black color indicates the carbon element and the white spots are the well-crystallized nickel elemental crystallite particles with uniform accumulative morphology, which can be seen in Figure 13.

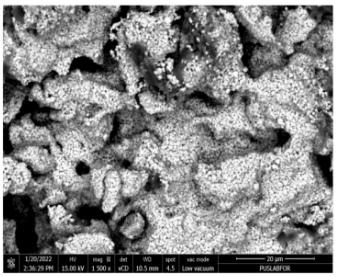

Figure 11. Micrograph of $LiNiO_2$ battery cathode material at a calcination time of 6 hours and a constant temperature of 700^0C

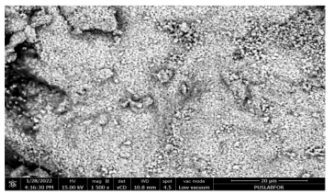

Figure 12. Micrograph of $LiNiO_2$ battery cathode material at a calcination time of 24 hours and a constant temperature of 700^0C

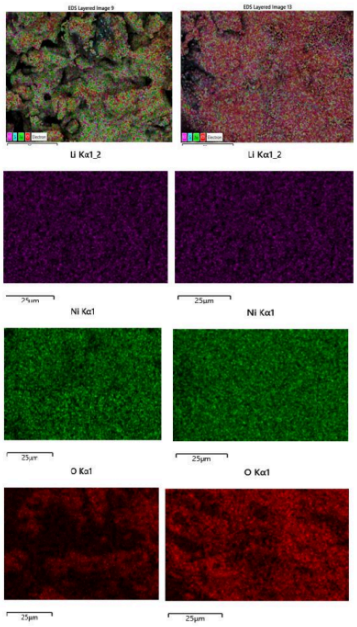

Figure 13. Surface morphology and distribution of elements of Lithium, Nickel, and Oxygen on the cathode material $LiNiO_2$ battery with calcination time of 6 hours and 24 hours, and a constant temperature of 700^0C

Table 4. Relationship of elemental composition to calcination time of cathode material $LiNiO_2$ battery

Elemental Content	Elemental composition (wt%)	
	Calcination time 6 Hours	Calcination time 24 Hours
Li	1,2	0,9
Ni	77,9	74,1
O	20,9	25,0

Figures 11 and 12, Surface morphology of the $LiNiO_2$ battery cathode material, shows that the crystallite particles are well crystallized with uniform accumulative morphology. This indicates that the crystallite particles from the synthesized samples have good morphology and the elemental composition of Lithium and Nickel elements decreases with the longer calcination time (Figure 13 and Table 4.). Because the presence of the element Ni^{2+} causes the position of the element Lithium (Li) to be swapped with the element Ni^{2+} so that the wrong atomic position can reduce the ability to move lithium ions and reduce the capacity of the battery. In addition, the presence of nitrate ions (NO_3) can help the oxidation process from Ni^{2+} to Ni^{3+} so that the phenomenon of the exchange of Li and Ni elements can be inhibited.

According to other researchers, the synthesized material with smaller particle size with high capacity and uniform particle size distribution improves the overall battery performance with uniform charge depth of each particle [12].

CONCLUSION

The results of calculations and analysis of the synthesis of $LiNiO_2$ battery cathode materials, using the single-stage co-precipitation method. Crystal structure testing using XRD showed that with increasing calcination time the mean crystallite diameter decreased (4.8961 nm to 1.0279 nm), but the average dislocation density increased (0.0538 lines/mm^2 to 1.8629 lines/mm^2). And the mean micro-lattice strain increased (2.0857% to 15.8079%) with the Miller hkl index (102), (104), (210), (108), and (113). Where the FTIR spectrum shows the vibration mode correlated with the vibrations of the octahedral units of NiO_6 and LiO_6 in the wavenumber zone of 400 - 700 cm^{-1}. Thus, the peak around 433 cm^{-1} is caused by the Li–O. Taken together, our experimental data help better understand the degradation processes, crystal imperfections (line defects), and inherent instability in the synthesis of $LiNiO_2$ as a lithium battery cathode material.

REFERENCES

[1] Sufriadin, "Extraction of Nickel and Cobalt from Sulawesi Limonite Ore in Nitric Acid Solution at Atmospheric Pressure," 2020. [Online]. Available: https://iopscience.iop.org/article/10.1088/1757-899X/875/1/012053

[2] V. F. Thomas, "Jokowi Sebut RI Strategis Jadi Produsen Baterai Lithium Dunia," 2020. [Online]. Available: https://tirto.id/jokowi-sebut-ri-strategis-jadi-produsen-baterai-litium-dunia-fXR7

[3] Shinichi Komaba, "Hydrothermal synthesis of high crystalline orthorhombic LiMnO2 as a cathode material for Li-ion batteries," *Solid*

State Ionics, vol. 152–153, pp. 311–318, 2002, [Online]. Available: https://www.sciencedirect.com/science/article/abs/pii/S016727380200320X

[4] Liu Yunjian, "Electrochemical performance and capacity fading reason of LiMn2O4/graphite batteries stored at room temperature," *J. Power Sources*, vol. 189, no. 1, pp. 721–725, 2009, [Online]. Available: https://www.sciencedirect.com/science/article/abs/pii/S0378775308016133

[5] Budiarto, "Laporan penelitian kelompok Pengaruh Temperatur Pemanasan Terhadap Struktur Kristal Dan Struktur Mikro Pada Sintesis Paduan LiNi 0,7Co0,2Fe0,1O2 Untuk Katoda Baterai Li-Ion," *Repository UKI*, 2021.

[6] R. Ibrahim Purawiardi, "Majalah Metalurgi," *Metalurgi*, vol. 31, no. 1, pp. 43–50, 2016.

[7] C. S. Yudha, "Synthesis and Characterization of Material LiNi0.8Co0.15Al0.05O2 Using One-Step Co-Precipitation Method for Li-Ion Batteries," *J. Kim. dan Pendidik. Kim.*, vol. 4, no. 3, pp. 134–144, 2019, [Online]. Available: https://jurnal.uns.ac.id/jkpk/article/view/29850

[8] H. Huang, "Approaching Theoretical Capacity of LiFePO4 at Room Temperature at High Rates," 2001. [Online]. Available: https://iopscience.iop.org/article/10.1149/1.1396695

[9] Wook Ahn, "Combustion-synthesized LiNi0.6Mn0.2Co0.2O2 as cathode material for lithium ion batteries," *J. Alloys Compd.*, vol. 609, pp. 143–149, 2014.

[10] H. Chen, "Effects of cationic substitution on structural defects in layered cathode materials LiNiO 2," *J. Mater. Chem. A*, vol. 2, pp. 7988– 7996, 2014.

[11] T. Hemida, "Green simple preparation of LiNiO2 nanopowder for lithium ion battery," *J. Mater. Res. Technol.*, vol. 9, no. 4, pp. 7955–7960, 2020.

[12] S. Kwon, "Effects of cathode fabrication conditions and cycling on the electrochemical performance of LiNiO 2 synthesized by combustion and calcination," *Ceram. Int.*, vol. 37, no. 5, pp. 1543–1548, 2011.

[13] P. Kalyani, "Various aspects of LiNiO2 chemistry: A review," *Sci. Technol. Adv. Mater.*, vol. 6, no. 6, pp. 689–703, 2005.

[14] Zengcai Liu, "Synthesis of LiNiO2 cathode materials with homogeneous Al doping at the atomic level," *J. Power Sources*, vol. 196, no. 23, pp. 10201–10206, 2011.

[15] Mutoa Shunsuke, "Effect of Mg-doping on the degradation of LiNiO2-based cathode materials by combined

spectroscopic methods," *J. Power Sources*, vol. 205, pp. 449–55, 2012.

[16] Y.-K. Sun, "Synthesis of Spinel LiMn2O4 by the Sol–Gel Method for a Cathode-Active Material in Lithium Secondary Batteries," *Solid State Ion*, vol. 156, pp. 319–328, 2003.

[17] Myoung Youp Song, "Synthesis by sol–gel method and electrochemical properties of LiNiO2 cathode material for lithium secondary battery," *J. Power Sources*, vol. 111, no. 1, pp. 97–103, 2002.

[18] B. R. Setiyadi and S. D. Ramdani, "Differences Of Seating Arrangements In Scientific Learning Approach In SMK," *J. Mech. Eng. Educ.*, vol. 1, no. 1, pp. 31–46, 2016.

[19] I. Bates, J. Clarke, P. Cohen, D. Finn, R. Moore, and P. Willis, *schooling for the dole*, I. Hampshire: MACMILLAN PUBLISHERS LTD, 1984.

Medyawanti Pane (Analysis of the Effect of Calcination Time on Microstructure, Functional Groups, and Crystal Structure of LiNiO2 Battery Cathode Material)

ORIGINALITY REPORT

18%	13%	11%	6%
SIMILARITY INDEX	INTERNET SOURCES	PUBLICATIONS	STUDENT PAPERS

PRIMARY SOURCES

1	eprints.uad.ac.id Internet Source	4%
2	e-jurnal.pnl.ac.id Internet Source	4%
3	N. Murali, S.J. Margarette, V. Kondala Rao, V. Veeraiah. "Structural, impedance, dielectric and modulus analysis ofLiNi 1-x-y-0.02 Mg 0.02 Co x Zn y O 2 cathode materials for lithium-ionbatteries", Journal of Science: Advanced Materials and Devices, 2017 Publication	2%
4	www.hindawi.com Internet Source	1%
5	lib.unnes.ac.id Internet Source	1%
6	Dewi Ratnasari, Agus Supriyanto. "Synthesis and characterization of lithium nickel cobalt aluminum cathode material from beverage can waste extracts", Journal of Physics: Conference Series, 2025 Publication	1%
7	dev.journal.ugm.ac.id Internet Source	1%
8	doaj.org Internet Source	1%
	dj.univ-danubius.ro	

9	Internet Source	1%
10	Muhammad Asif. "Handbook of Energy Transitions", CRC Press, 2022 Publication	<1%
11	www.buzzle.com Internet Source	<1%
12	ejournal2.pnp.ac.id Internet Source	<1%
13	d-nb.info Internet Source	<1%
14	Submitted to New York Institute of Technology Student Paper	<1%
15	S DHAMEJA. "Electric Vehicle Batteries", Electric Vehicle Battery Systems, 2002 Publication	<1%
16	Submitted to University of Newcastle Student Paper	<1%
17	newatlas.com Internet Source	<1%
18	www.ourenergypolicy.org Internet Source	<1%
19	www.studysmarter.co.uk Internet Source	<1%
20	patents.justia.com Internet Source	<1%
21	Arif Jumari, Enni Apriliyani, Soraya Ulfa Muzayanha, Agus Purwanto, Adrian Nur. "Reprocessing through co-precipitation of NCA cathode scrap waste for cathode material of Li-ion battery", AIP Publishing, 2020 Publication	<1%

22	Brian L. Ellis, Linda F. Nazar. "Sodium and sodium-ion energy storage batteries", Current Opinion in Solid State and Materials Science, 2012 Publication	<1 %
23	G Nagasubramanian, R.G Jungst, D.H Doughty. "Impedance, power, energy, and pulse performance characteristics of small commercial Li-ion cells", Journal of Power Sources, 1999 Publication	<1 %
24	studentsrepo.um.edu.my Internet Source	<1 %
25	www.austceram.com Internet Source	<1 %
26	Shuhui Sun, Xueliang Sun, Zhongwei Chen, Yuyu Liu, David P. Wilkinson, Jiujun Zhang. "Carbon Nanomaterials for Electrochemical Energy Technologies - Fundamentals and Applications", CRC Press, 2017 Publication	<1 %
27	Miyeon Jang, Gwangyong Yi, Hyeonjin Jeon, Chungsik Yoon. "Current Status of Processes and Hazardous Chemicals of Lithium-ion Battery Industries in the Republic of Korea", Safety and Health at Work, 2024 Publication	<1 %

Exclude quotes	On	Exclude matches	Off
Exclude bibliography	On		